HHS Public Access

Author manuscript

J Invest Dermatol. Author manuscript; available in PMC 2018 March 01.

Published in final edited form as:

J Invest Dermatol. 2017 March ; 137(3): 576–586. doi:10.1016/j.jid.2016.09.033.

A Topical Mitochondria-Targeted Redox Cycling Nitroxide Mitigates Oxidative Stress Induced Skin Damage

Rhonda M. Brand[1,2], **Michael W. Epperly**[3], **J. Mark Stottlemyer**[1,2], **Erin M. Skoda**[4], **Xiang Gao**[5], **Song Li**[5], **Saiful Huq**[3], **Peter Wipf**[4,5,7], **Valerian E. Kagan**[6], **Joel S. Greenberger**[3], and **Louis D. Falo Jr**[1,7]

[1]Department of Dermatology, University of Pittsburgh, Pittsburgh, Pennsylvania 15213, USA

[2]Department of Medicine, University of Pittsburgh, Pittsburgh, Pennsylvania 15213, USA

[3]Department of Radiation Oncology, University of Pittsburgh, Pittsburgh, Pennsylvania 15213, USA

[4]Department of Chemistry, University of Pittsburgh, Pittsburgh, Pennsylvania 15213, USA

[5]Department of Pharmaceutical Sciences, University of Pittsburgh, Pittsburgh, Pennsylvania 15213, USA

[6]Department of Environmental and Occupational Health, University of Pittsburgh, Pittsburgh, Pennsylvania 15213, USA

[7]Department of Bioengineering, University of Pittsburgh, Pittsburgh, Pennsylvania 15213, USA

Abstract

Skin is the largest human organ and provides a first line of defense that includes physical, chemical, and immune mechanisms to combat environmental stress. Radiation is a prevalent environmental stressor. Radiation induced skin damage ranges from photoaging and cutaneous carcinogenesis from UV exposure, to treatment-limiting radiation dermatitis associated with radiotherapy, to cutaneous radiation syndrome, a frequently fatal consequence of exposures from nuclear accidents. The major mechanism of skin injury common to these exposures is radiation induced oxidative stress. Efforts to prevent or mitigate radiation damage have included development of antioxidants capable of reducing reactive oxygen species (ROS). Mitochondria are particularly susceptible to oxidative stress, and mitochondrial dependent apoptosis plays a major role in radiation induced tissue damage. We reasoned that targeting a redox cycling nitroxide to mitochondria could prevent ROS accumulation, limiting downstream oxidative damage and preserving mitochondrial function. Here we show that in both mouse and human skin, topical application of a mitochondrial targeted antioxidant prevents and mitigates radiation induced skin damage characterized by clinical dermatitis, loss of barrier function, inflammation, and fibrosis.

Corresponding Author: Louis D. Falo, Jr., M.D., Ph.D., Department of Dermatology, University of Pittsburgh, 200 Lothrop Street, Presby South Tower, Suite 3880, Pittsburgh, PA 15213, Phone: 412-864-3664, Fax: 412-864-3734, lof2@pitt.edu.

Further, damage mitigation is associated with reduced apoptosis, preservation of the skin's antioxidant capacity, and reduction of irreversible DNA and protein oxidation associated with oxidative stress.

Keywords

oxidative stress; antioxidant; radiation dermatitis; UVR carcinogenesis; photoaging

INTRODUCTION

ROS and reactive nitrogen species (RNS) are generated in the skin by UVA (Opländer and Suschek, 2013), UVB (Terra et al., 2012), visible (Liebel et al., 2012), infrared (Svobodová and Vostálová, 2010), and ionizing radiation (Liauw et al., 2013). Under conditions of oxidative stress, accumulating ROS/RNS deplete the skin's innate antioxidant capacity (Valacchi et al., 2012). Supra-physiologic ROS cause widespread oxidative damage cascades that include lipid peroxidation, protein carbonylation, and DNA damage through strand breaks and DNA-protein crosslinking. ROS are also pro-inflammatory, with direct effects on transcription factors regulating the inflammatory cascade and indirect effects via release of pro-inflammatory damage-associated molecular patterns (DAMPs) in response to oxidative stress induced tissue damage (Janko et al., 2012). Increasing evidence suggests that effects of early radiation induced oxidative stress lead to chronic oxidative stress that contributes to late tissue injury (Azzam et al., 2012). Mitochondria are a major intracellular source of oxidants and are particularly susceptible to ROS (Azzam et al., 2012). Oxidative damage leads to disruption of the critical interaction between mitochondrial cardiolipin and cytochrome c, activating the intrinsic mitochondrial apoptotic pathway. Release of cytochrome c from the inner mitochondrial membrane is associated with activation of caspase 3, PARP, and apoptosis (Sinha et al., 2013).

Therapeutic agents that scavenge ROS can potentially act upstream of the oxidative stress damage cascade to prevent or mitigate radiation damage. TEMPOL (4-hydroxy-2,2,6,6-tetramethylpiperidinyloxy) is a redox cycling nitroxide that promotes the metabolism of many ROS and improves nitric oxide bioavailability in a concentration-dependent manner (Circu and Aw, 2010; Hahn et al., 1992; Mitchell et al., 1991). To improve the intracellular/mitochondrial partitioning of TEMPOL and thereby increase its effective concentration, we conjugated TEMPOL to a fragment of gramicidin S that displays significant affinity for the inner mitochondrial membrane. The resulting 4-amino TEMPOL conjugate, XJB-5-131 (MW 958.2), was further optimized to improve its physicochemical properties, resulting in JP4-039 (MW 424.6) (Bernard et al., 2011; Frantz et al., 2011; Greenberger et al., 2012; Skoda et al., 2012; Wipf et al., 2005). JP4-039 partitions preferentially into mitochondria, resulting in enhanced drug efficiency vs. common antioxidants including TEMPOL (Bernard et al., 2011; Goff et al., 2011; Greenberger et al., 2012).

To evaluate the radioprotective effect of JP4-039, we first utilized a mouse model of radiation damage in which the shaved skin is selectively exposed to radiation with a limited depth of penetration (Janko et al., 2012). This produces severe oxidative stress in the skin

and damage similar to that expected from the direct deposition of particulate fallout β-particles. The resulting β-burn is characterized by erythema early on followed by trans-epithelial injury (moist desquamation), ulceration, and necrosis (Williams et al., 2010). In this model, ROS generation in the skin exceeds that from UV exposure or fractionated radiotherapy, and enables a stringent evaluation of strategies to prevent or mitigate skin damage from oxidative stress (Azzam et al., 2012).

RESULTS

We initially sought to evaluate mitochondrial targeting and biologic activity of topically applied JP4-039 in the skin using Electron Paramagenetic Resonance Spectroscopy (EPR). EPR detects absorption of electromagnetic radiation by a sample containing one or more unpaired electrons placed in a magnetic field of a defined frequency (Hawkins and Davies, 2014) and has been used to confirm XJB-5-131 and JP4-039 mitochondrial targeting in a variety of cell lines and tissues (Epperly et al., 2010; Rajagopalan et al., 2009; Wipf et al., 2005). EPR is well suited to determine the presence and distribution of EPR-active therapeutic and mitigating agents in biological systems (Pristov et al., 2011). The presence of an unpaired electron enables nitroxides to display a distinctive and characteristic triplet signal that is proportional to the concentration present in the sample (Fink et al., 2007).

To confirm the effective targeting of JP4-039 to mitochondria in intact skin after topical application, JP4-039 and TEMPO (Sigma) were formulated with a lipid carrier, formulation F-14, at a concentration of 4 mg/ml and a drug to carrier weight ratio of 1:50 (w/w) (Goff et al., 2011), and applied to the depilated backs of mice for 30 minutes. Cytosolic and mitochondrial fractions were isolated from skin biopsies by differential centrifugation, and electron paramagnetic resonance (EPR) was used to determine partitioning of JP4-039 (Roy et al., 2009). In JP4-039 treated skin, the characteristic triplet EPR signal typical of the JP4-039 nitroxide radical was present in the unfractionated skin homogenate and the mitochondrial fraction, and absent in the cytosol (Fig 1a), consistent with preferential mitochondrial localization. Quantification of EPR spectra and comparison of JP4-039 to untargeted TEMPOL confirmed JP4-039 localization in the mitochondria, whereas TEMPO was found principally in the cytosol (Fig 1b). Further, detection of the nitroxide signal by EPR verified its biologic activity in these cells. To visually confirm the presence of JP4-039 in the mitochondria, JP4-039-Bodipy was synthesized (Bernard et al., 2011; Frantz et al., 2013) and applied to mouse skin as described above. Skin sections (Fig 1c) and isolated keratinocytes (Fig 1d) were labeled with Mitotracker Red-CMXROS and DAPI and analyzed by confocal microscopy (600X). Merged samples confirmed the localization of JP4-039-Bodipy in the mitochondria (Fig 1c,d).

In initial studies to assess the efficacy of skin protection, groups of mice were irradiated with 35 Gy and treated by topical application of JP4-039 or formulation alone 0.5, 24 and 48 h after exposure, or left untreated. 21 days after irradiation, untreated and groups treated with formulation alone (controls) demonstrated characteristic β-burns with severe desquamation and ulceration at the irradiation site. In contrast, the skin of JP4-039 treated mice was intact, with minimal erythema (Fig. 2a). To support this subjective clinical assessment of skin damage, we evaluated skin function using two distinct quantitative measures. First, to

quantitatively evaluate skin barrier function, we measured Transepidermal Water Loss (TEWL). This non-invasive metric measures the rate of water evaporation from the skin surface, with increasing TEWL values correlating to increasing compromise of the skin's barrier function (Bergeron et al., 2012; Brand and Jendrzejewski, 2008). Consistent with clinical appearance, irradiated control groups demonstrated severe compromise in skin barrier function. In contrast, JP4-039 treatment preserved skin barrier function at near normal levels (Fig. 2b). As a second functional measure we evaluated leg extension. Changes in leg contraction are a functional marker of increased collagen levels and fibrosis, and damage is quantitated as the stretching differential between control and irradiated legs (Stone, 1984). Irradiation reduces stretching capacity, as evidenced by greater differences in extension between the treated and untreated legs of irradiated control mice, compared to unirradiated mice (Fig 2c). Mice treated with JP4-039 demonstrated significantly less contraction injury (Fig 2c). Consistent with this, histological assessment demonstrated that JP4-039 treatment reduced collagen deposition in the skin (Fig. 2d), and dermal (Fig. 2e,f) and epidermal thickening (Fig. 2e,g) typically associated with cutaneous radiation damage. Similarly, JP4-039 significantly reduced the inflammatory infiltrate in the skin that is seen in irradiated groups (Fig. 2e,h) and in radiation damaged skin in general (Flanders et al., 2002).

To directly evaluate the effects of radiation induced oxidative stress at the cellular and molecular levels, mice were irradiated with 35 Gy, and then treated or not with JP4-039 or formulation 0.5 h after irradiation. Mice were euthanized 4 h after irradiation and skin harvested for analysis. Radiation induced inflammatory infiltrates were evident at this early time point in irradiated control skin, but absent in JP4-039 treated skin (Fig. 3a,c). We evaluated radiation induced apoptosis histologically by TUNEL assay and enzymatically by caspase release (Yin et al., 2013). By both measures, JP4-039 significantly reduced radiation-induced apoptosis (Fig. 3b,d,e), which was most pronounced in the epidermis histologically (Fig. 3b). To directly measure the antioxidant effects of JP4-039, we compared levels of glutathione (GSH), the most abundant antioxidant present in the skin, in irradiated skin with or without JP4-039 treatment (Valacchi et al., 2012). Radiation significantly depleted GSH levels in skin in untreated and formulation only treated skin, compared to unirradiated controls (Fig. 3f). Irradiated skin treated with JP4-039 maintained GSH levels observed in unirradiated normal skin, demonstrating the potent antioxidant capacity of topical JP4-039 (Fig. 3f). Consistent with this antioxidant effect, JP4-039 treatment significantly reduced oxidative stress induced DNA damage as measured by 8-oxoguanine immunohistochemistry (Azzam et al., 2012; Cadet and Douki, 2011) (Fig. 3g).

Anatomic and physiologic differences between murine and human skin emphasize the importance of human-tissue based preclinical modeling of potential radioprotective agents before clinical trials. To this end, we have developed a human skin explant model comprised of intact, living, and physiologically active human skin. These human skin organ cultures are derived from normal freshly excised de-identified human skin and maintain their integrity and viability in culture for more than 10 days. To evaluate radiation induced oxidative stress and damage in human skin, skin explants were irradiated with 60 Gy, a dose that generates substantial ROS and is equivalent to the cumulative exposure of patients undergoing fractionated therapy for head and neck cancer (Liauw et al., 2013). Skin samples were irradiated, treated or not 30 min later with formulation only or JP4-039, and then harvested

for analysis after 24h of culture at 37 °C at the air-fluid interface. Representative histology is shown for each of these 4 conditions (Fig. 4a). We evaluated radiation induced apoptosis histologically by TUNEL and enzymatically by caspase release as described previously. Apoptosis was substantial in irradiated untreated or formulation treated skin compared to un-irradiated controls (Fig. 4b,d,e). Importantly, by both measures, treatment with JP4-039 significantly reduced radiation-induced apoptosis (Fig. 4b,d,e). To directly measure the antioxidant effects of JP4-039, we compared levels of glutathione in irradiated skin with or without JP4-039 treatment. As observed in the mouse models, radiation significantly depleted GSH levels in skin in untreated and formulation treated skin, compared to un-irradiated controls (Fig. 4f). Irradiated skin treated with JP4-039 maintained GSH levels that were not significantly different from those found in un-irradiated normal skin, demonstrating the potent antioxidant capacity of topical JP4-039 in human skin (Fig. 4f). Importantly, JP4-039 treatment significantly reduced oxidative stress induced DNA damage as measured by 8-oxoguanine immunohistochemistry in human skin (Fig. 4c,g). Further, while irradiation resulted in substantial oxidative stress induced protein carbonylation (Azzam et al., 2012; Doctrow et al., 2013; Yanagihara et al., 2013) in untreated and formulation treated skin, JP4-039 protected proteins in the skin from oxidative damage as evidenced by the absence of carbonylated proteins which remained at negligible un-irradiated baseline levels (Fig. 4h). Taken together, these results demonstrate that JP4-039 applied topically to human skin reduces apoptosis, preserves the skin's antioxidant capacity, and protects the skin from irreversible DNA and protein oxidation associated with severe oxidative stress.

In some applications, the capacity of a therapeutic agent to reverse or neutralize radiation induced damage when administered well after the exposure event will be critical to its efficacy (Singh et al., 2012). In the case of antioxidants, such mitigation of radiation damage is feasible, as damage from oxidative stress is progressive and cumulative, and has even been implicated in late tissue injury from radiation exposure (Azzam et al., 2012). To evaluate the capacity of topical JP4-039 to mitigate skin damage from radiation induced oxidative stress, we repeated our previous murine studies, but delayed JP4-039 application until 24h after radiation. Specifically, groups of mice were irradiated with 35 Gy and treated by topical application of JP4-039 or formulation alone 24, 48, and 72h after exposure, or left untreated. Twenty one days after irradiation, untreated and formulation only controls again demonstrated characteristic β-burns with severe desquamation and ulceration at the irradiation site. In contrast, and as observed in the preventive setting, the skin of JP4-039 treated mice was intact, with minimal erythema (Fig. 5a). Consistent with clinical appearance, irradiated untreated and formulation treated groups demonstrated severe compromise in skin barrier function as measured by TEWL, while JP4-039 significantly preserved skin barrier function, with treated groups having near normal skin barrier function (Fig. 5b). Similarly, mice treated with JP4-039 demonstrated significantly less contraction injury (Fig 5c). As observed in the protection setting, histological assessment was consistent with these functional results. JP4-039 treatment reduced collagen deposition in the skin (Fig. 5d), and dermal (Fig. 5e,f) and epidermal thickening (Fig. 5e,g) typically associated with cutaneous radiation damage. Further, JP4-039 applied topically 24 h after irradiation mitigated the inflammation present in the skin of irradiated control groups (Fig. 5h). By these clinical, functional, and histologic criteria, JP4-039 applied topically 24 h after

radiation exposure was as effective in mitigating skin damage from radiation induced oxidative stress as it was in protecting the skin when applied within 30 min of radiation exposure (Fig. 2).

DISCUSSION

UV and ionizing radiation induce cutaneous effects with clinical and mechanistic similarities. In both cases, acute radiation induced skin injury results in alterations in the epidermis and dermis that include erythema, impaired skin barrier function, inflammation, and pigment changes. Late manifestations of radiation damage depend on the balance between the magnitude of the initial insult and endogenous compensatory mechanisms, and can range from telangiectasias and other manifestations characteristic of photoaging, to fibrosis, ulceration, and carcinogenesis (Ryan, 2012; Sklar et al., 2013). Mechanistically, both UV and ionizing radiation induce oxidative stress, inflammation, and direct DNA damage including characteristic base pair deletions (Gordon-Thomson et al., 2012; Krishnan and Birch-Machin, 2005; Peng et al., 2006; Zhao and Robbins, 2009). Radiation induced ROS deplete skin antioxidants, disrupting the balance between naturally occurring pro and anti-oxidants, eventually overwhelming the skin's natural antioxidant capacity. Excess ROS result in oxidation of lipids, carbohydrates, and proteins, and oxidative damage of DNA primarily through 8-oxoguanine modifications that increase the frequency of spontaneous mutations (Cadet and Douki, 2011; Svobodová and Vostálová, 2010; Tulah and Birch-Machin, 2013; Yirmibesoglu et al., 2012). The direct and oxidative DNA damage generated by both forms of radiation contribute to immunosuppression and reduce immunosurveillance, in part through impairment of the antigen presenting capabilities of dendritic cells present in the skin (Kripke, 2013; Ryan, 2012).

Mitochondria are particularly susceptible to damage from radiation induced oxidative stress. Oxidative stress induced mechanisms activate the intrinsic mitochondrial apoptotic pathway resulting in cell death. Radiation induced ROS damage mitochondrial proteins, a process which is generally irreversible and is measured by the formation of carbonyl groups on lysine, proline, arginine and threonine residues (Banfi et al., 2008; Pleshakova et al., 1998). Mitochondrial DNA (mtDNA) located in the matrix attached to the inner mitochondrial membrane is directly exposed to ROS. mtDNA is particularly susceptible to damage as a result of a combination of factors including - an absence of introns that results in more than 95% coding sequences, the absence of protective histones, and the absence of nucleotide excision repair mechanisms present in nuclear DNA (Tulah and Birch-Machin, 2013). Based on this rationale, we reasoned that mitochondrial targeting of an electron scavenging agent could potentially result in sufficiently high mitochondrial concentration of ROS scavengers to prevent the oxidative stress damage cascade, thereby protecting mitochondria and reducing radiation induced cell death.

We have previously shown that JP4-039, a gramicidin S conjugated nitroxide, is a potent electron scavenging agent that displays significant affinity for the inner mitochondrial membrane compared to common antioxidants, increasing its functional concentration in mitochondria (Bernard et al., 2011; Goff et al., 2011; Greenberger et al., 2012). Administered systemically, JP4-039 can improve survival of mice exposed to lethal ionizing

radiation (Epperly et al., 2010; Goff et al., 2011). Here, we demonstrate the remarkable potential of JP4-039 as a topical antioxidant. In both mouse and human skin, our results demonstrate that topical JP4-039, applied at the time of radiation exposure (prevention) or afterward (mitigation) significantly reduces the clinical manifestations of radiation induced skin damage. We demonstrate that JP4-039 accumulates in the mitochondria of skin cells by EPR and fluorescence measurements. Importantly, our studies systematically demonstrate potent antioxidant effects at clinical, histologic, cellular and molecular levels. Topical JP4-039 preserves the skin's antioxidant capacity, as indicated by reductions in oxidative stress driven GSH depletion. JP4-039 treatment reduces radiation induced ROS damage to DNA reflected by reduced 8-oxoG modifications, and proteins as indicated by the absence of protein carbonylation in treated skin. Overall, JP4-039 treatment results in a substantial reduction in apoptosis in treated skin as measured histologically by TUNEL assay and enzymatically by caspase assay. Other histologic evidence of effectiveness includes reduced collagen deposition, reduction in epidermal and dermal thickening, and decreases in inflammatory infiltrates. These observations correlate with clinical and functional measures of effectiveness including reduction of dermatitis by image analysis, preserved barrier function by TEWL measurement, and reduced fibrosis measured by leg extension.

Importantly, we demonstrated the effectiveness of topical JP4-039 under conditions of radiation exposure that produce severe oxidative stress, even to the point of producing a β-burn. Under these conditions, levels of radiation induced ROS in the skin exceed those caused by UV exposure or fractionated radiotherapy (Azzam et al., 2012). Further, in addition to demonstrating the protective effects of topical JP4-039 in the skin of living mice, we extended this analysis to demonstrate effectiveness in living human skin. As there are distinct anatomic and functional differences between mouse and human skin, this human-tissue based preclinical modeling critically supports the feasibility of future clinical trials.

Development of a topical antioxidant capable of protecting the skin from damage from radiation induced oxidative stress would have broad applications for skin health. An effective topical antioxidant could reduce the incidence of UV induced skin cancers and prevent or delay photoaging. UVR induces carcinogenic DNA damage both directly by induction of DNA photoproducts, and indirectly through absorption by non-DNA chromophores that generate ROS responsible for oxidative DNA damage, including oxidized DNA bases such as 8-oxo-guanine (Seebode et al., 2016). Further, UVA induced ROS induces extensive protein oxidation, including potentially the inactivation of essential DNA repair proteins. A recent study demonstrates that DNA repair, including nucleotide excision repair, is inhibited by UVA induced ROS (McAdam et al., 2016). By reducing UVA induced ROS, redox cycling nitroxides could help preserve nucleotide excision repair mechanisms, preventing the accumulation of directly induced mutations. In addition to well established links between UV induced oxidative stress and skin cancer, there is also an established link between UVR induced ROS production, mtDNA damage, and skin aging that supports the use of the mitochondrial targeted redox cycling nitroxides for the prevention or treatment of photoaging (Anderson et al., 2014). In this context, it has been suggested that ROS induced mtDNA damage in the skin could be a useful tool for screening therapeutic antioxidants (Oyewole et al., 2014). The role of mitochondrial damage in UVR induced skin damage and in diverse skin diseases (Feichtinger et al., 2014, Boulton et al., 2015) and the protective

mechanisms of mitochondrial targeted antioxidants (Oyewole et al., 2015) have recently been reviewed. Finally, it is important to note that there are currently no evidenced based interventions to ameliorate radiation induced skin damage in the setting of radiotherapy (Singh et al., 2016). Our results with JP4-039 suggest that topical antioxidants applied before or during radiotherapy could reduce the incidence of radiation dermatitis, reducing morbidity and improving therapeutic efficacy by reducing treatment interruptions and enabling more effective treatment regimens. Taken together, studies presented here provide strong support for future clinical trials designed to determine the therapeutic potential of topical JP4-039 in these and related clinical applications.

METHODS

Chemical synthesis and formulation

JP4-039 was synthesized in the laboratory of P. Wipf at the University of Pittsburgh as previously described (Wipf et al., 2005) and dispersed in PBS with the help of a lipid carrier, formulation F-14 (sesame oil: egg yolk phosphatidylcholine: tween 80: span 85 = 50:25:12.5:12.5 w:w), at a concentration of 2 mg/ml and a drug to carrier weight ratio of 1:50 (w/w) (Goff et al., 2011). A brief sonication with an energy output of 10 W was used to reduce the particle sizes to approximately 250 nm. Control F-14 formulation was prepared identically but contains no drug.

Irradiation procedure

All C57BL/6NHsd mice were maintained in an AAALAC approved facility and were treated according to the NIH Guide for the Care and Use of Laboratory Animals. Approximately 24h prior to irradiation the right rear leg of each mouse was shaved and the depilatory agent Nair was applied to the bare skin. Three minutes after application the Nair was washed off and the mice were allowed to recover. Approximately 5 min prior to irradiation, each mouse was anesthetized by injecting 1.25 mg/kg of Nembutal. A 6 MeV electron beam from a Varian 23EX linear accelerator was used to generate beta-irradiation burns. Irradiation was conducted using a 25 cm x 25 cm applicator, a dose rate of 1000 MU/min and a source-to-mouse skin surface distance of 100 cm. A specifically designed cutout with five 2cm x 2cm openings, each separated from the other by solid cerrobend alloy, was fabricated to enable five mice to be irradiated simultaneously. During irradiation, five mice were placed side-by-side on a 3 cm thick bolus. The setup is such that only the shaved upper right rear leg of each mouse is exposed to an irradiation field of 2cm x 2cm. All monitor units were calculated by incorporating the appropriate applicator factor and cut-out factors such that the doses delivered to mouse skin was 35 Gy. Control mice received sham irradiation. For prevention studies 0.5, 24 and 48h after irradiation 50uL of the radio-mitigating agent JP4-039 or formulation alone were topically applied to the skin. In a second study designed to test mitigating capacities, the same quantity of JP4-039 was applied at 24, 48 and 72h post irradiation.

Human skin explants

De-identified discarded freshly excised human skin samples were irradiated with 60 Gy as described above and were cultured as raft cultures epidermal-side up on top of sterile

stainless steel mesh screens (0.1 mm pore) placed inside 6 well plates containing serum-free Aim V medium as previously described (Killeen et al., 2013; Larregina et al., 2001a; Larregina et al., 2001b; Morelli et al., 2005). Skin explants were cultured sterilely at the liquid air interface for 24h. Skin explants were irradiated as described. Thirty minutes after irradiation 50μL of JP4-039 or formulation alone were topically applied to groups of skin explants as detailed in the text.

EPR analysis of partitioning and distribution of nitroxides in the skin

Nitroxide partitioning of JP4-039 into subcellular compartments was determined with electron paramagnetic resonance (EPR). Liposomes containing 4mg/mL of JP4-039 or TEMPO (Sigma) were applied to the depilated backs of mice for 30 minutes. The skin was thoroughly washed and skin biopsies were homogenized. To isolate subcellular compartments by differential centrifugation the homogenate was centrifuged at 900xG for 10 min at 4 °C. The supernatant was then centrifuged at 10,000xG for 15 min at 4 °C and collected as the cytosolic fraction. The pellet containing the mitochondria was then washed gently with 2 mL PBS and centrifuged at 10,000xG for 4 min at 4 °C (Roy et al., 2009).

Subcellular fractions were mixed with dimethyl sulfoxide (DMSO) (1:1 v/v) and 2 mM of potassium ferricyanide to convert nitroxides to EPR-detectable radical forms (23). EPR measurements were made with a JEOL-RE2X EPR spectrometer (Jeol, Tokyo, Japan) with the following settings: center field, 335.0 mT; sweep width, ±5.0 mT; frequency, 9.4 GHz; microwave power, 20 mW; sweep rate, 0.23 min/mT; field modulation, 0.079; response time 0.1 sec. Using the signal magnitude and isolated volumes, the concentration of JP4-039 or TEMPO were calculated for each sample (Wipf et al., 2005).

Visualization of JP-Bodipy in mitochondria

JP-Bodipy was synthesized as described previously (Bernard et al., 2011; Frantz et al., 2013) and incorporated into liposomes as described earlier. Liposomes containing 4 mg/mL of Bodipy conjugated JP4-039 were applied to the shaved backs of mice for 30 min, and skin was processed and biopsied as described above. Skin was cultured in 50uM Mitotracker Red-CMXROS (Life Technologies M-7512) for 30 minutes, frozen in OCT and cut in 8uM sections. Samples were then fixed and nuclei were stained with DAPI prior to photographing with confocal microscope (600X). Merged samples confirm localization of JP4-039-Bodipy in the mitochondria. For isolated keratinocytes, the epidermis was isolated by incubating skin dermal side down in 0.3% trypsin at 37 °C for 90 min, followed by manual disaggregation. Epidermal cells were plated on a coated coverslip and allowed to attach for 24 h. After washing, cells were DAPI stained as described above.

Skin barrier function

TEWL measurements were determined with a VapoMeter (SWL, Delfin Kuopio, Finland) using the standard adaptor with an 11mm diameter opening as previously described (Brand and Jendrzejewski, 2008). Data were normalized with the average reading at 35 GY set to 100% and from 0 GY control mice to 0% using GraphPad Prism (GraphPad, La Jolla, CA) algorithm.

Leg contracture

A jig was constructed that enabled accurate measurement of maximal leg extension for each leg (Stone, 1984). Differential leg extension is defined as extension in the control leg minus extension in irradiated leg, with a higher difference indicating greater damage.

Collagen deposition

Biopsy samples were placed in 10% formalin for 24 h, bisected along the longitudinal axis, embedded in paraffin and cut into 5um sections. Relative collagen levels were assed using Masson's Trichrome staining. Slides were examined by a dermatopathologist for signs of fibrosis.

Inflammation and damage

Skin sections were evaluated for signs of inflammation and skin damage via hematoxylin and eosin (H&E) stains, by measuring dermal and epidermal thickening and cellular infiltrate using the methods described in Flanders et al (Flanders et al., 2002). For epidermal thickness, 5 images were taken of each slide at 200x, starting with an area of interfolicular acanthosis and photographing four adjacent fields. Epidermal thickness was measured from the outer edge to the epidermal-dermal interface using Image J Software (NIH). Five measurements were taken of each image and the 5 images were averaged to determine an average for each slide. Dermal thickness was measured in a similar manner, except photos were taken at 100X and distance from the dermal-epidermal junction and fatty layer were obtained. Cellular infiltrate was determined by counting the number of cells in a 100,000 pixel area (400X) on each of five images per slide. An average of each of the five images resulted in a single value per animal.

Apoptosis

Paraffin embedded sections were analyzed by TUNEL assay (DermaTACS, Trevigen, Gaithersburg MD) counterstained with Nuclear Red (Vector Laboratories, Burlingame CA). Cell death was quantitated by photographing four consecutive fields. The percent of apoptotic cells was determined by counting the number of epidermal blue apoptotic cells and dividing by the total number of epidermal cells in the field. In addition to the histologic assessment described above, we quantitatively evaluted apoptosis by measuring caspase-3 activity in the supernatant of homogenized tissue samples using the luminescence Caspase-GloR 3/7 assay kit (Promega, Madison, WI). Three 6 mm punch biopsies were homogenized in 300 μl of PBS+2mM EDTA and were centrifuged at 1000 g for 10 min. Results were normalized to mg tissue for mouse skin and mg protein for human skin.

Oxidative stress

Glutathione (GSH) levels were estimated in supernatants from skin homogenates using GSH –glo assay kit (Promega, Madison, WI). Results were normalized to mg tissue for mouse skin and mg protein for human skin.

Carbonyl protein levels were determined using the OxyElisa kit (Millipore, #S7250, Billerica, MA). Homogenized skin protein concentration was determined by staining with

coomassie. Oxyelisa plates were coated overnight at 4 °C with skin homogenate supernatants diluted to a protein concentration of 0.025 μg/mL in Lysis Buffer. Oxyelisa assay was performed following the Millipore protocol.

DNA damage was determined by assessing 8h-hydroxyguanosine by immunohistochemistry. Slides were deparrafinized and rehydrated. Antigen retrieval was performed using sodium citrate buffer and 0.1% trypsin according to manufacturer's protocol (Abcam). Slides were blocked, stained with Polyclonal Goat anti 8-Hydroxyguanosine primary antibody (Abcam, ab10802), stained with Horseradish Peroxidase conjugated Rabbit anti-Goat IgG (Abcam, ab6741) and developed with 3,3′ Diaminobenzidine (Dab) substrate kit (Abcam, ab64238) according to manufacturer's protocol with the exception of a 1 min incubation with the Dab.

Statistics

Data were converted to % change from control which is defined as (Treated/Control − 1) *100 and then presented as mean + s.e.m. Statistical differences were determined via 1 way ANOVA followed by a Bonferonni Post-Test with $p<0.05$ set for statistical significance. All calculations were performed using GraphPad Prism (GraphPad, La Jolla, CA).

Study Approval

All mouse experiments were approved by the University of Pittsburgh IACUC committee. All human samples were procured in accordance with Declaration of Helsinki protocols and University of Pittsburgh Institutional Review Board approval. Informed consent was received prior to human tissue acquisition.

Acknowledgments

The authors would like to thank Rachel Cline, Tracy Dixon and Dr. Adrianna Larregina for their technical assistance. This project received support from the NIH/NIGMS CMLD program (P50 GM067082), CMCR program (U19-A1068021), and NIAID (1RC1AI081284). Drs. Greenberger, Epperly, and Falo are inventors of related intellectual property covered by patents. The authors state no other conflicts.

Abbreviations

ROS	Reactive Oxygen Species
TEWL	Transepidermal Water Loss
UV	Ultraviolet
GSH	glutathione
TEMPOL	4-hydroxy-2,2,6,6-tetramethylpiperidinyloxy
Gy	gray

References

Azzam EI, Jay-Gerin J-P, Pain D. Ionizing radiation-induced metabolic oxidative stress and prolonged cell injury. Cancer Letters. 2012; 327(1–2):48–60. [PubMed: 22182453]

Anderson A, Bowman A, Boulton SJ, Manning P, Birch-Machin MA. A role for human mitochondrial complex II in the production of reactive oxygen species in human skin. Redox Biol. 2014; 2C:1016–1022.

Banfi C, Brioschi M, Barcella S, Veglia F, Biglioli P, Tremoli E, et al. Oxidized proteins in plasma of patients with heart failure: role in endothelial damage. Eur J Heart Fail. 2008; 10(3):244–51. [PubMed: 18331966]

Bergeron L, Gondran C, Oberto G, Garcia N, Botto JM, Cucumel K, et al. Skin presenting a higher level of caspase-14 is better protected from UVB irradiation according to in vitro and in vivo studies. J Cosmet Dermatol. 2012; 11(2):111–21. [PubMed: 22672275]

Bernard ME, Kim H, Berhane H, Epperly MW, Franicola D, Zhang X, et al. GS-nitroxide (JP4-039)-mediated radioprotection of human Fanconi anemia cell lines. Radiat Res. 2011; 176(5):603–12. [PubMed: 21939290]

Boulton SJ, Bowman A, Koohgoli R, Birch-Machin MA. Skin manifestations of mitochondrial dysfunction: more important than previously thought. Exp Dermatol. 2015; 24(1):12–3. [PubMed: 25403780]

Brand RM, Jendrzejewski JL. Chronic ethanol ingestion alters xenobiotic absorption through the skin: potential role of oxidative stress. Food Chem Toxicol. 2008; 46(6):1940–8. [PubMed: 18336981]

Cadet J, Douki T. Oxidatively generated damage to DNA by uva radiation in cells and human skin. J Invest Dermatol. 2011; 131(5):1005–7. [PubMed: 21494240]

Circu ML, Aw TY. Reactive oxygen species, cellular redox systems, and apoptosis. Free radical biology & medicine. 2010; 48(6):749–62. [PubMed: 20045723]

Doctrow SR, Lopez A, Schock AM, Duncan NE, Jourdan MM, Olasz EB, et al. A synthetic superoxide dismutase/catalase mimetic euk-207 mitigates radiation dermatitis and promotes wound healing in irradiated rat skin. J Invest Dermatol. 2013; 133(4):1088–96. [PubMed: 23190879]

Epperly MW, Goff JP, Li S, Gao X, Wipf P, Dixon T, et al. Intraesophageal administration of gs-nitroxide (jp4-039) protects against ionizing irradiation-induced esophagitis. In Vivo. 2010; 24(6): 811–9. [PubMed: 21164038]

Feichtinger RG, Sperl W, Bauer JW, Kofler B. Mitochondrial dysfunction: a neglected component of skin diseases. Exp Dermatol. 2014; 23(9):607–14. [PubMed: 24980550]

Fink MP, Macias CA, Xiao J, Tyurina YY, Jiang J, Belikova N, et al. Hemigramicidin-TEMPO conjugates: novel mitochondria-targeted anti-oxidants. Biochem Pharmacol. 2007; 74(6):801–9. [PubMed: 17601494]

Flanders KC, Sullivan CD, Fujii M, Sowers A, Anzano MA, Arabshahi A, et al. Mice lacking Smad3 are protected against cutaneous injury induced by ionizing radiation. The American journal of pathology. 2002; 160(3):1057–68. [PubMed: 11891202]

Frantz M-C, Skoda EM, Sacher JR, Epperly MW, Goff JP, Greenberger JS, et al. Synthesis of analogs of the radiation mitigator JP4-039 and visualization of BODIPY derivatives in mitochondria. Organic & biomolecular chemistry. 2013; 11(25):4147–53. [PubMed: 23715589]

Frantz, M-Cl, Pierce, JG., Pierce, JM., Kangying, L., Qingwei, W., Johnson, M., et al. Large-scale asymmetric synthesis of the bioprotective agent jp4-039 and analogs. Organic Letters. 2011; 13(9): 2318–21. [PubMed: 21452836]

Goff JP, Epperly MW, Dixon T, Wang H, Franicola D, Shields D, et al. Radiobiologic effects of gs-nitroxide (jp4-039) on the hematopoietic syndrome. In Vivo. 2011; 25(3):315–23. [PubMed: 21576404]

Gordon-Thomson C, Gupta R, Tongkao-on W, Ryan A, Halliday GM, Mason RS. 1a,25 Dihydroxyvitamin D3 enhances cellular defences against UV-induced oxidative and other forms of DNA damage in skin. Photochemical & Photobiological Sciences. 2012; 11(12):1837–47. [PubMed: 23069805]

Greenberger JS, Clump D, Kagan V, Bayir H, Lazo JS, Wipf P, et al. Strategies for discovery of small molecule radiation protectors and radiation mitigators. Frontiers in Oncology. 2012:1.

Hahn SM, Tochner Z, Krishna CM, Glass J, Wilson L, Samuni A, et al. Tempol, a stable free radical, is a novel murine radiation protector. Cancer research. 1992; 52(7):1750–3. [PubMed: 1551104]

Hawkins CL, Davies MJ. Detection and characterisation of radicals in biological materials using EPR methodology. Biochim Biophys Acta. 2014; 1840(2):708–21. [PubMed: 23567797]

Janko M, Ontiveros F, Fitzgerald TJ, Deng A, DeCicco M, Rock KL. IL-1 Generated Subsequent to Radiation-Induced Tissue Injury Contributes to the Pathogenesis of Radiodermatitis. Radiation Research. 2012; 178(3):166–72. [PubMed: 22856653]

Killeen ME, Ferris L, Kupetsky EA, Falo L, Mathers AR. Signaling through purinergic receptors for atp induces human cutaneous innate and adaptive th17 responses: Implications in the pathogenesis of psoriasis. The Journal of Immunology. 2013; 190(8):4324–36. [PubMed: 23479230]

Kripke ML. Reflections on the field of photoimmunology. J Invest Dermatol. 2013; 133(1):27–30. [PubMed: 22854621]

Krishnan KJ, Birch-Machin MA. The incidence of both tandem duplications and the common deletion in mtdna from three distinct categories of sun-exposed human skin and in prolonged culture of fibroblasts. J Invest Dermatol. 2005; 126(2):408–15.

Larregina AT, Morelli AE, Spencer LA, Logar AJ, Watkins SC, Thomson AW, et al. Dermal-resident CD14+ cells differentiate into Langerhans cells. Nat Immunol. 2001a; 2(12):1151–8. [PubMed: 11702065]

Larregina AT, Watkins SC, Erdos G, Spencer LA, Storkus WJ, Beer Stolz D, et al. Direct transfection and activation of human cutaneous dendritic cells. Gene Ther. 2001b; 8(8):608–17. [PubMed: 11320407]

Liauw SL, Connell PP, Weichselbaum RR. New paradigms and future challenges in radiation oncology: An update of biological targets and technology. Science Translational Medicine. 2013; 5(173):173sr2. [PubMed: 23427246]

Liebel F, Kaur S, Ruvolo E, Kollias N, Southall MD. Irradiation of skin with visible light induces reactive oxygen species and matrix-degrading enzymes. J Invest Dermatol. 2012

McAdam E, Brem R, Karran P. Oxidative stress-induced protein damage inhibits DNA repair and determines mutation risk and therapeutic efficacy. Mol Cancer Res. 2016 pii: molcanres. 0053.2016. [Epub ahead of print].

Mitchell JB, DeGraff W, Kaufman D, Krishna MC, Samuni A, Finkelstein E, et al. Inhibition of oxygen-dependent radiation-induced damage by the nitroxide superoxide dismutase mimic, tempol. Archives of biochemistry and biophysics. 1991; 289(1):62–70. [PubMed: 1654848]

Morelli AE, Rubin JP, Erdos G, Tkacheva OA, Mathers AR, Zahorchak AF, et al. Cd4+ T cell responses elicited by different subsets of human skin migratory dendritic cells. The Journal of Immunology. 2005; 175(12):7905–15. [PubMed: 16339526]

Opländer C, Suschek C. The role of photolabile dermal nitric oxide derivates in ultraviolet radiation (uvr)-induced cell death. International Journal of Molecular Sciences. 2013; 14(1):191–204.

Oyewole AO, Wilmot MC, Fowler M, Birch-Machin MA. Comparing the effects of mitochondrial targeted and localized antioxidants with cellular antioxidants in human skin cells exposed to UVA and hydrogen peroxide. FASEB J. 2014; 28(1):485–94. [PubMed: 24115050]

Oyewole AO, Birch-Machin MA. Mitochondria-targeted antioxidants. FASEB J. 2015; 29(12):4766–71. [PubMed: 26253366]

Peng TI, Yu PR, Chen JY, Wang HL, Wu HY, Wei YH, et al. Visualizing common deletion of mitochondrial DNA-augmented mitochondrial reactive oxygen species generation and apoptosis upon oxidative stress. Biochim Biophys Acta. 2006; 1762(2):241–55. [PubMed: 16368227]

Pleshakova OV, Kutsyi MP, Sukharev SA, Sadovnikov VB, Gaziev AI. Study of protein carbonyls in subcellular fractions isolated from liver and spleen of old and gamma-irradiated rats. Mechanisms of ageing and development. 1998; 103(1):45–55. [PubMed: 9681878]

Pristov JB, Mitrovic A, Spasojevic I. A comparative study of antioxidative activities of cell-wall polysaccharides. Carbohydrate research. 2011; 346(14):2255–9. [PubMed: 21880306]

Rajagopalan MS, Gupta K, Epperly MW, Franicola D, Zhang X, Wang H, et al. The mitochondria-targeted nitroxide JP4-039 augments potentially lethal irradiation damage repair. In Vivo. 2009; 23(5):717–26. [PubMed: 19779106]

Roy P, Nigam N, George J, Srivastava S, Shukla Y. Induction of apoptosis by tea polyphenols mediated through mitochondrial cell death pathway in mouse skin tumors. Cancer Biology & Therapy. 2009; 8(13):1281–7. [PubMed: 19556852]

Ryan JL. Ionizing Radiation: The good, the bad, and the ugly. J Invest Dermatol. 2012; 132(3):985–93. [PubMed: 22217743]

Seebode C, Lehmann J, Emmert S. Photocarcinogenesis and Skin Cancer Prevention Strategies. Anticancer Res. 2016; 36(3):1371–8. [PubMed: 26977038]

Singh M, Alavi A, Wong R, Akita S. Radiodermatitis: A Review of Our Current Understanding. [Epub ahead of print]. Am J Clin Dermatol. [accessed 28 March 2016]

Singh VK, Ducey EJ, Brown DS, Whitnall MH. A review of radiation countermeasure work ongoing at the Armed Forces Radiobiology Research Institute. International Journal of Radiation Biology. 2012; 88(4):296–310. [PubMed: 22191567]

Sinha K, Das J, Pal P, Sil P. Oxidative stress: the mitochondria-dependent and mitochondria-independent pathways of apoptosis. Arch Toxicol. 2013:1–24.

Sklar LR, Almutawa F, Lim HW, Hamzavi I. Effects of ultraviolet radiation, visible light, and infrared radiation on erythema and pigmentation: a review. Photochemical & Photobiological Sciences. 2013; 12(1):54–64. [PubMed: 23111621]

Skoda EM, Davis GC, Wipf P. Allylic amines as key building blocks in the synthesis of (E)-alkene peptide isosteres. Org Process Res Dev. 2012; 16(1):26–34. [PubMed: 22323894]

Stone HB. Leg contracture in mice: an assay of normal tissue response. International journal of radiation oncology, biology, physics. 1984; 10(7):1053–61.

Svobodová A, Vostálová J. Solar radiation induced skin damage: Review of protective and preventive options. International Journal of Radiation Biology. 2010; 86(12):999–1030. [PubMed: 20807180]

Terra VA, Souza-Neto FP, Pereira RC, Xavier Da Silva TN, Ramalho LNZ, Luiz RC, et al. Nitric oxide is responsible for oxidative skin injury and modulation of cell proliferation after 24 hours of UVB exposures. Free Radical Research. 2012; 46(7):872–82. [PubMed: 22512358]

Tulah AS, Birch-Machin MA. Stressed out mitochondria: The role of mitochondria in ageing and cancer focussing on strategies and opportunities in human skin. Mitochondrion. 2013; 13(5):444–53. [PubMed: 23195682]

Valacchi G, Sticozzi C, Pecorelli A, Cervellati F, Cervellati C, Maioli E. Cutaneous responses to environmental stressors. Annals of the New York Academy of Sciences. 2012; 1271(1):75–81. [PubMed: 23050967]

Williams JP, Brown SL, Georges GE, Hauer-Jensen M, Hill RP, Huser AK, et al. Animal models for medical countermeasures to radiation exposure. Radiat Res. 2010; 173(4):557–78. [PubMed: 20334528]

Wipf P, Xiao J, Jiang J, Belikova NA, Tyurin VA, Fink MP, et al. Mitochondrial targeting of selective electron scavengers: Synthesis and biological analysis of hemigramicidin–TEMPO conjugates. Journal of the American Chemical Society. 2005; 127(36):12460–1. [PubMed: 16144372]

Yanagihara S, Kobayashi H, Tamiya H, Tsuruta D, Okano Y, Takahashi K, et al. Protective effect of hochuekkito, a Kampo prescription, against ultraviolet B irradiation-induced skin damage in hairless mice. The Journal of Dermatology. 2013; 40(3):201–6. [PubMed: 23294358]

Yin Y, Li W, Son Y-O, Sun L, Lu J, Kim D, et al. Quercitrin protects skin from UVB-induced oxidative damage. Toxicology and Applied Pharmacology. 2013

Yirmibesoglu E, Karahacioglu E, Kilic D, Lortlar N, Akbulut G, Omeroglu S. The protective effects of ginkgo biloba extract (EGb-761) on radiation-induced dermatitis: an experimental study. Clinical and Experimental Dermatology. 2012; 37(4):387–94. [PubMed: 22211952]

Zhao W, Robbins MEC. Inflammation and chronic oxidative stress in radiation-induced late Normal tissue injury: Therapeutic implications. Current Medicinal Chemistry. 2009; 16(2):130–43. [PubMed: 19149566]

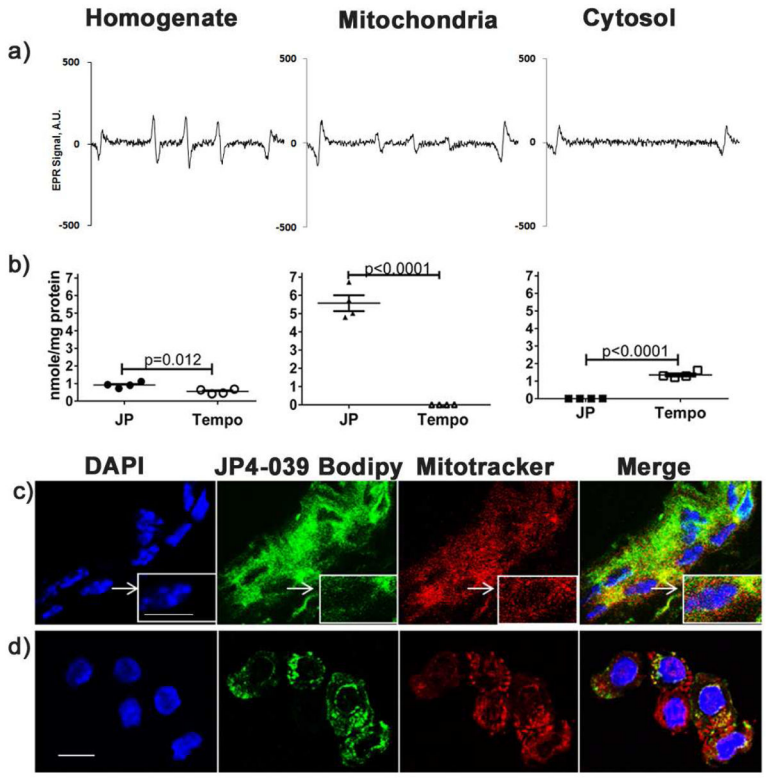

Figure 1. Topical JP4-039 localizes to keratinocyte mitochondria

Whole skin homogenates and subcellular fractions were derived from mouse skin 30 min after topical application of JP4-039 or Tempo. Typical EPR spectra of JP4-039 nitroxide radical in unfractionated cell homogenates and mitochondrial and cytosolic subfractions are shown (**a**). EPR spectra were used to quantitate levels of nitroxide radicals present in each fraction in JP4-039 or Tempol treated skin (n=4) (**b**). JP4-039 bodipy treated intact skin (**c**) and isolated keratinocytes (**d**) were labeled with Mitotracker Red-CMXROS and Dapi and imaged by confocal microscopy. Merged images confirm localization of JP4-039-Bodipy in the mitochondria (bar=10μm. Statistical significance was determined using a t-test.

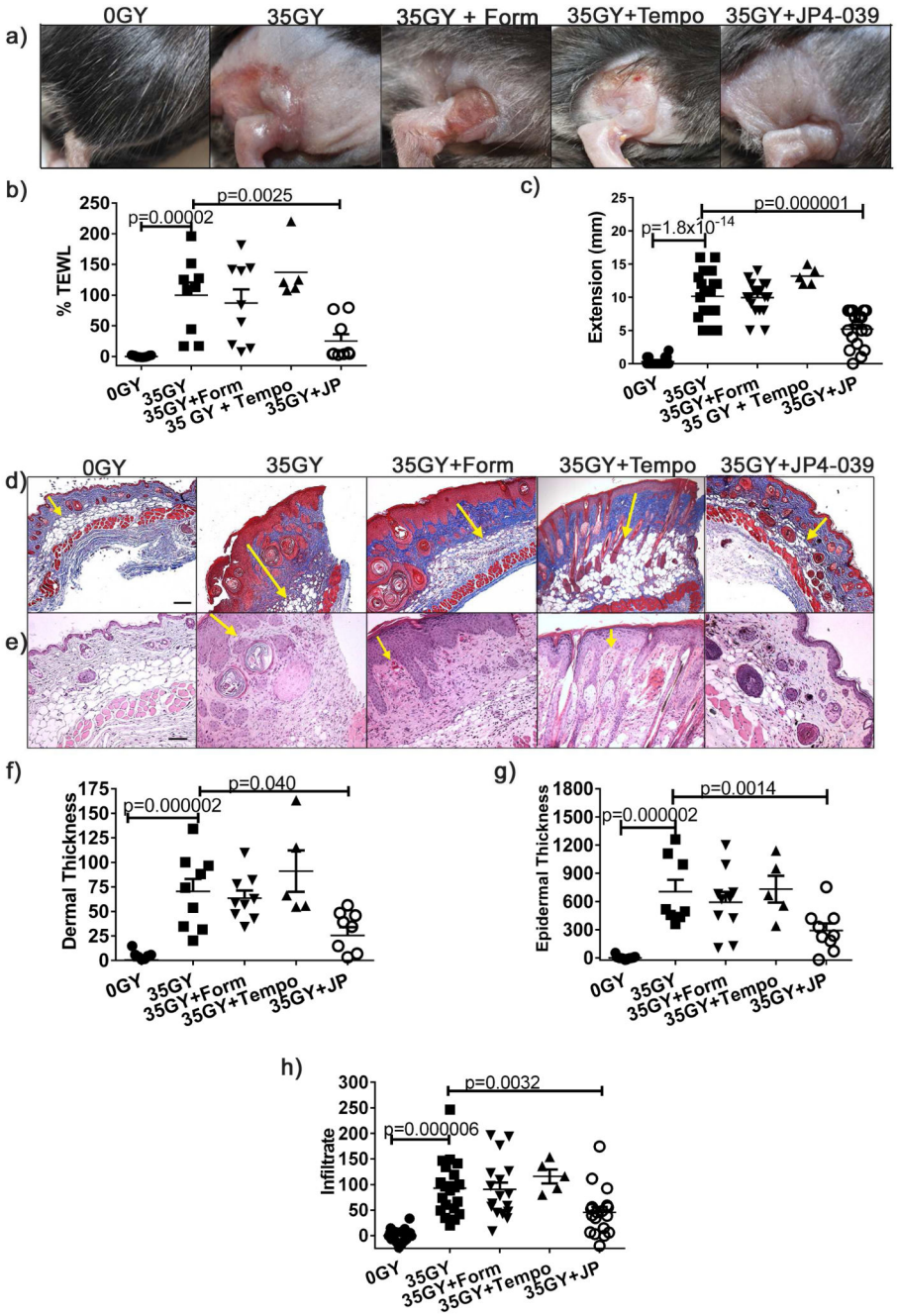

Figure 2. Topical JP4-039 prevents skin damage from radiation induced oxidative stress

Mice were irradiated with 35 Gy and left untreated or treated topically with JP4-039 or formulation alone 0.5, 24 and 48 h after irradiation. Shown are representative clinical photographs 21 days post-irradiation are shown (**a**), skin barrier function determined with TEWL (**b**), differences between extension of irradiated and non-irradiated legs (**c**) and collagen fibers (**d**) (bar = 80μm). Representative H&E stained sections are provided in (**e**) with arrows delineating dermal and epidermal thickness (bar = 40μm). Dermal (**f**) 100X) and epidermal (**g**) thickness (200X) were measured. Infiltrating cells in 400X sections were

counted (**h**). All data are presented as mean ± SEM (n=10–20). Statistical significance was determined by ANOVA followed by a Bonferroni post-test set at $p<0.05$.

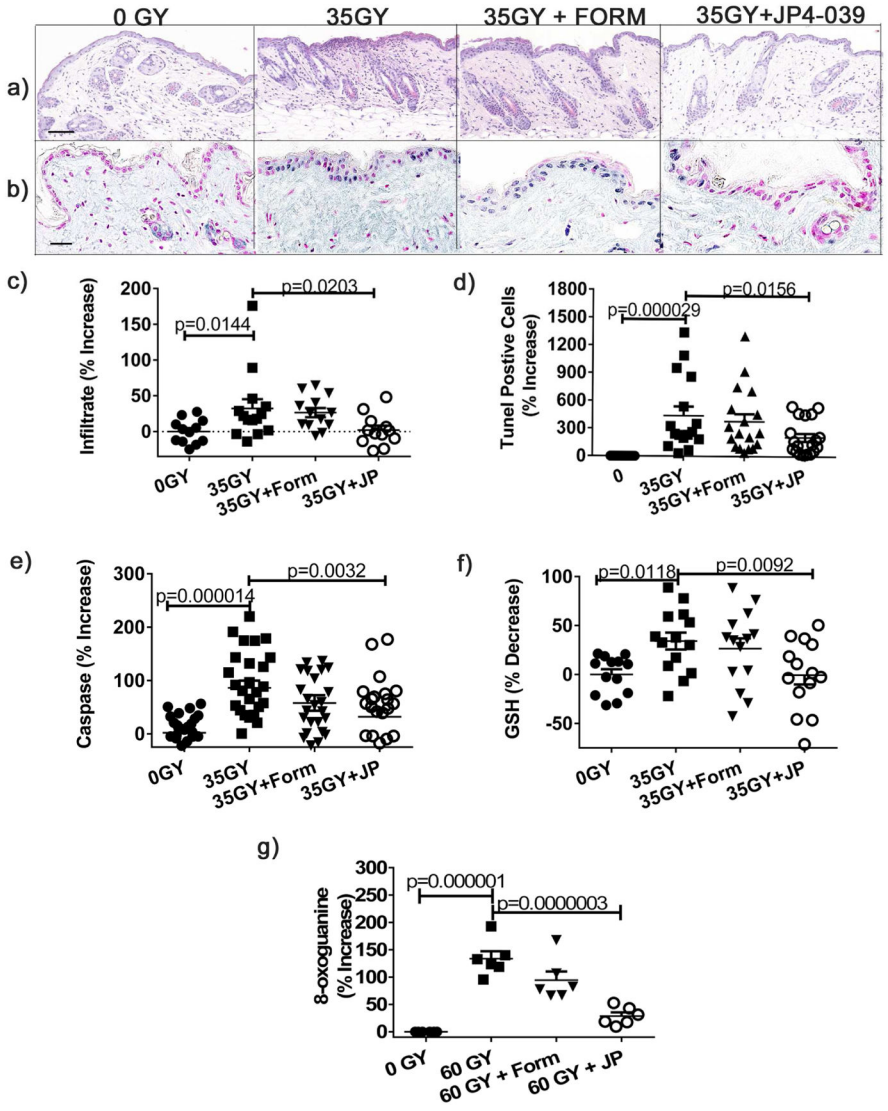

Figure 3. Topical JP4-039 prevents radiation induced cutaneous apoptosis, inflammation, antioxidant depletion, and DNA damage

35 Gy irradiated mice were treated or not 0.5h after irradiation. Shown are representative H&E sections 4 h after irradiation (bar = 40μm) (**a**), quantified cellular infiltrates (**b**), TUNEL stained sections (**b**) with positive cells staining blue and negative cells red (bar = 20μm), quantification of TUNEL positive cells (**d**), and Caspase 3/8 levels determined in homogenates (**e**). GSH levels were determined enzymatically from skin homogenates (**f**). DNA damage was evaluated by 8-oxoguanine staining and expressed as percent positive cells (**g**). Results are presented as % increase (((treated/untreated average)−1)*100). Data are presented as mean ± SEM (n=13–22). Statistical significance was determined by ANOVA followed by a Bonferroni post-test with significance set at $p<0.05$.

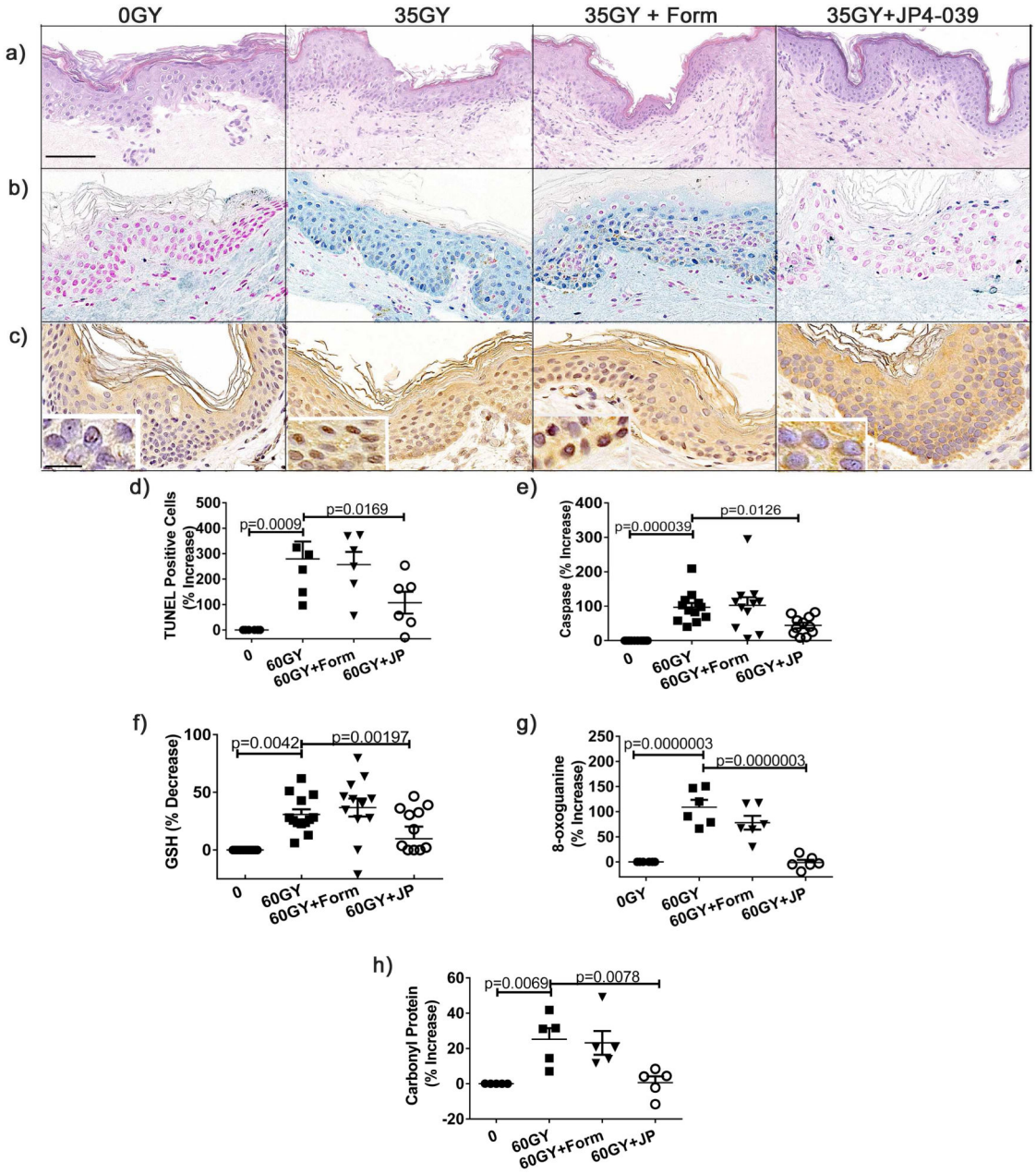

Figure 4. JP4-039 applied to human skin demonstrates potent antioxidant function and prevents skin damage from radiation induced oxidative stress

60 Gy Irradiated human skin was treated topically with JP4-039 or not 30 min after irradiation and harvested 24h later for analysis. Depicted are H&E stained sections (bar = 40μm) (a), apoptosis as determined by TUNEL (b), percent positive TUNEL cells (d), and Caspase 3/7 levels (e). GSH levels were determined enzymatically (f). DNA damage was determined by 8-oxoguanine antibody (inset bar = 10μm) (c), and percentage of positive cells quantitated (g). Carbonyl protein levels were determined by ELISA (h). Data were analyzed as described in Figure 3.

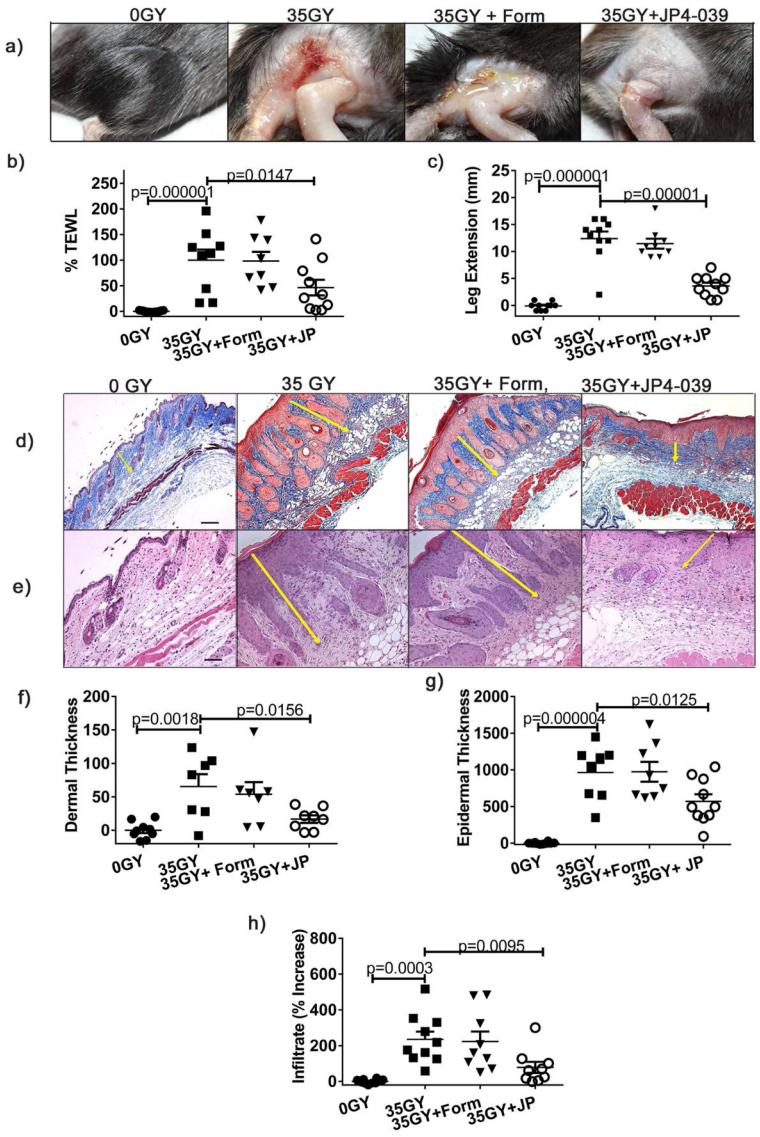

Figure 5. Topical JP4-039 mitigates skin damage from radiation induced oxidative stress

Mice were irradiated with 35 Gy and left untreated or treated topically with JP4-039 or formulation alone 24, 48 and 72h after irradiation. Representative clinical photographs from 21 days post-irradiation are shown (**a**). Changes in skin barrier function were determined with TEWL (**b**). Differences between extension of irradiated and non-irradiated legs is a functional measure of fibrosis (**c**). Collagen fibers identified with Masson's Trichrome staining (bar = 80μm) (**d**). Representative H&E stained sections are provided in (**e**) with arrows delineating dermal and epidermal thickness (bar = 40μm). Dermal (**f**) (100X) and epidermal (**g**) thickness (200X) were measured. Infiltrating cells in 400X section were counted (**h**). Data were analyzed as described in Figure 2.